Ain Shams Engineering Journal 15 (2024) 102364

Contents lists available at ScienceDirect

Ain Shams Engineering Journal

journal homepage: www.sciencedirect.com

Compact linearly polarized 5G Vivaldi non-uniform slot filtering antenna

Sahar Saleh [a,b,*], Nick Timmons [a], Jim Morrison [a], Widad Ismail [c]

[a] WiSAR Lab, Atlantic Technological University (ATU), Letterkenny, Co. Donegal F92 FC93, Ireland
[b] Department of Electronics and Communications Engineering, Faculty of Engineering, Aden University, Aden 5243, Yemen
[c] School of Electrical and Electronic Engineering, Universiti Sains Malaysia, Nibong Tebal, Penang 14300, Malaysia

ARTICLE INFO

Article history:
Received 24 February 2023
Revised 8 May 2023
Accepted 9 June 2023
Available online 28 June 2023

Keywords:
Filtering antenna (filtenna)
Vivaldi non-uniform slot filtering antenna (VNSFA)
Hairpin bandpass filter (HPBF)
5G
Mobile communication

ABSTRACT

This research proposes compact linearly polarized 5G Vivaldi non-uniform slot filtering antennas (VNSFAs) with stable radiation patterns and improved bandwidth (BW) and gain. The 5G third-order uniform transmission line hairpin bandpass filter (UTL HPBF) is first designed, and a 17.17 % size reduction is obtained using the non-uniform transmission line (NTL) theory. Secondly, the Vivaldi non-uniform slot profile antenna (VNSPA) theory is applied to design the UWB compact VNSA with 51.94 % size reduction, 2.91 %, and 5.8 % BW and gain enhancement. Finally, the predesigned compact UWB VNSA's good performance is exploited in this work to be integrated with the compact 5G UTL and NTL HPBFs using a co-design methodology resulting in novel compact 6.55 GHz VNSFAs. These VNSFAs are compatible with modern wireless system miniaturization requirements. They are also considered good candidates for cognitive radio networks (CRNs) to mitigate spectrum scarcity. In this work, simulations are carried out using computer simulation technology (CST) software and they are validated by comparing them to the measured results. VNSFAs using UTL and NTL HPBFs provide measured S_{11} of <−10.35 dB and <−10.34 dB at 5.6–7.76 GHz and 6–7.76 GHz with peak realized gains of 4.84 dBi and 5.23 dBi, respectively. The obtained findings prove the effectiveness of using the simple and low-cost compactness techniques of NTL and VNSPA theories in reducing the filtenna size without degrading its performance.

1. Introduction

Recent development in communication systems and the dependency on Internet-of-Things (IoT), increase the number of devices used. To fulfill the requirement of secure, fast, and large data transmission rates of modern applications, fifth-generation (5G) technology is used offering enhanced, ultra-reliable, and low-latency communication.

To meet the commercial demand for small devices with lower power consumption and cost, antennas and filters should be conveniently integrated into the communication system [1]. The first concept of a filtering antenna (filtenna) was proposed in [2] and [3] by combining the antenna and filter in one module (co-design approach) and replacing the filter's last resonator with a radiator (synthesis approach), respectively. Although more compactness can be achieved by etching slots or adding parasitic elements to the antenna [4], they may degrade the antenna's performance. However, filters provide more controllable procedures on the required band-edge selectivity, and high-order harmonics suppression [5].

Using a co-design approach, circularly polarized square patch and circularly polarized monopole antennas are combined with two coupled stripline open-loop resonator bandpass filters (BPFs) [6,7] and two-stage split ring resonator (SRR) [8], respectively for off body wireless communication. For the application of wearable devices, wireless sensors, active RFID readers, and other IoT's gadgets, a two-stage SRR is integrated with a linearly polarized monopole antenna [9]. However, for wireless communication devices, multimode stub-loaded resonators (SLRs) are integrated with low-profile slot antenna [10]. A parasitic element with slits and BPF are integrated with the Vivaldi antenna to control its beamwidth and maximum gain for directional communication, imaging, and sensing at 28 GHz for upcoming 5G base stations and fixed terminals [11]. An elliptic-shaped monopole filtenna for satellite com-

* Corresponding author at: WiSAR Lab, Atlantic Technological University (ATU), Letterkenny, Co. Donegal F92 FC93, Ireland.
E-mail addresses: sahar.saleh@atu.ie (S. Saleh), nick.timmons@atu.ie (N. Timmons), jim.morrison@atu.ie (J. Morrison), eewidad@usm.my (W. Ismail).
Peer review under responsibility of Ain Shams University.

Production and hosting by Elsevier

https://doi.org/10.1016/j.asej.2023.102364
2090-4479/

munication, global positioning system (GPS), and aviation surveillance system applications is designed exploiting the interdigital bandpass filter's (IBPF) superior selectivity and harmonics suppression capabilities [12].

However, for the synthesis approach, the second resonator of a square capacitively loaded loop (CLL) and square open loop resonator (SOLR) filters are replaced by a fan-shaped radiator [13] and inverted L-shape monopole antenna [14] to enhance selectivity and to be used for Wi-Fi application, respectively. For compactness, high selectivity, and high degrees rejection levels, multilayer structures are used where a load-insensitive multimode balun filter (back-to-back coupled patches) and three microstrip SOLRs are integrated into a quasi-Yagi [15] and Γ`-shaped [16] antennas. In order to improve the filtennas' level of selectivity recommended for current wireless communication systems [17], wireless local area network (WLAN), and power harvest applications [18], differential feeding structures are utilized. A novel leaky-wave filtenna with a wide bandwidth (36.36 %) and high gain (8.65 dBi) and >13 dB out-of-band suppression is designed using spoof surface plasmon polaritons (SSPPs) and double-sided parallel strip line (DSPSL) [19]. For portable 5G mid-band (3.6–3.8 GHz) devices, compact low-cost filtenna is proposed by integrating a CLL into a crescent-shaped planar monopole antenna [20]. Reconfigurable filtenna utilizing the proper switching mechanisms are used to enhance the radio system's flexibility and reliability. A useful review of reconfigurable antennas for 5G wireless and CubeSat applications can be found in [21]. For microwave breast imaging applications, a switchable filter impulse radio ultra-wideband (IR-UWB) filtenna is designed using square-shaped filters integrated into the partial ground plane of a CPW-fed wideband cylindrical shape antenna [22]. Using a modified quarter-wave monopole (arrow-shaped) antenna with filtering stub and pin diodes, reconfigurable filtenna is designed for global system for mobile communication (GSM), fourth generation long-term evolution (4G-LTE), industrial, scientific and medical (ISM), and 5G Sub-6 GHz band applications [23]. Four varactor diodes are installed in the integrated BPF of the wideband (1.3–3 GHz) monopole antenna to enable tunable operation from 2.7 GHz to 2 GHz for cognitive radio network (CRN) applications [24]. In [25] authors proposed two reconfigurable filtennas for CRN application. Three slots with three pin diodes are added to the UWB patch antenna to control the notch at WLAN, X, and International Telecommunication Union (ITU) bands. However, five pin diodes are used to tune the antenna between C-band, WLAN, or X-band regions for UWB sensing. Recently, in [26], the compact 5G low-frequency band (5.975–7.125 GHz) UTL [27] and NTL [28,29] hairpin bandpass filters (HPBFs) are combined with the proposed compact UWB (3.1–10.6 GHz) Vivaldi tapered slot antenna (VTSA) [30] resulting in a compact 5G Vivaldi tapered slot filtering antennas (VTSFAs) with improved bandwidth (BW), and gain.

In this work, the compact 5G UTL [27] and NTL [28,29] HPBFs are integrated with the proposed compact linearly polarized UWB (3.1–10.6 GHz) VNSA [31] exploiting its good UWB performance (high gain, wide BW and stable radiation patterns) resulting in a compact 5G (5.975–7.125 GHz) Vivaldi non-uniform slot filtering antennas (VNSFAs) with 51.94 % size reduction as compared to VTSFA in [26]. The 5G low-frequency band (5.975–7.125 GHz) was proposed by Federal Communications Commission (FCC) for unlicensed operation in 5G. To enhance the spectrum efficiency of the wireless communication system, the proposed VNSFAs are good candidates for CRNs applying suitable switching mechanisms using the same concept in [32]. Future work may include using the techniques in the recently proposed compact UTL and NTL IBPFs [33] to achieve smaller sizes with wider BW and to eliminate the HPBFs' higher-order harmonic problems. In this paper, Antenna 1 and Antenna 2 refer to VNSFA based on UTL, and NTL HPBFs, respectively. In addition to this section, Section 2 describes the optimal design of the proposed filtenna, and Section 3 discusses the results.

2. Design and analysis

The proposed compact 5G (5.975–7.125 GHz) Antenna 1 and 2 are achieved by integrating the compact 5G UTL [27] and NTL [28,29] HPBFs with the compact UWB (3.1–10.6 GHz) VNSA [31]. The purpose of choosing the Vivaldi antenna is to exploit its good characteristics in terms of easy integration with other circuits (the UTL and NTL HPBFs in this work), moderate-high gain, wide BW, and stable radiation patterns. The VNSA [31] is chosen in this work owing to its 51.94 % size reduction, 2.91 %, and 5.8 % bandwidth and maximum realized gain improvement as compared to VTSA [30]. UTL and NTL HPBFs are chosen to get the required 5G low-frequency band (5.975–7.125 GHz) by suppressing undesirable signals and offering more space for switches and DC biasing circuits [32] in CRNs application using NTL HPBF with 17.17 % size reduction. The substrate, Rogers RO4003C with εr = 3.55, height (h) = 0.813 mm, dielectric loss tangent of 0.0027, and copper thickness = 0.035 mm is used in this study.

The 5G (5.975–7.125 GHz) UTL HBPF is designed based on the design equations in [34] using a Chebyshev lowpass prototype with a passband ripple of 0.1 dB and $g_0 = g_4 = 1$, $g_1 = g_3 = 1.0316$, $g_2 = 1.1474$. Then its size is reduced by 17.17 % by applying the NTL theory [28,29,35–37] resulting in NTL HBPF. The steps for designing these filters are briefly illustrated in Fig. 1 where Fc and FBW are the center frequency and fractional BW, respectively.

However, the linearly polarized UWB VNSA is designed by applying the new VNSPA theory developed in [31] to reduce the size of compact UWB VTSA [30] where its tapper slot profile (TSP) with length (L_T), varying characteristics impedance $Z_T(x)$ (varying width $W_T(x)$) and propagation constant $\beta_T(x)$ is replaced by nonuniform slot profile (NSP) with a 33.33 % reduced length (L_N), varying characteristics impedance $Z_N(x)$ (varying width $W_N(x)$) and propagation constant $\beta_N(x)$ as shown in Fig. 2. According to [31], both profiles will be equivalent if their ABCD parameters are equal conditioning that their aperture opening (W_{min}) and width (W_{max}) are equal. TSP and NSP are defined respectively as follows

$$W_T(x) = \pm Ae^{r*x} \tag{1}$$

$$ln(W_N(x)/W_T(x)) = \sum_{n=0}^{N} C_n \cos\left(\frac{2\pi n x_N}{L_N}\right) \tag{2}$$

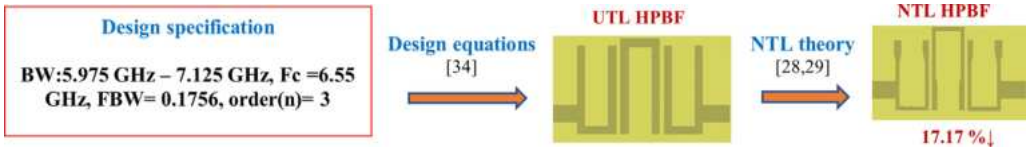

Fig. 1. UTL and NTL HPBFs design steps.

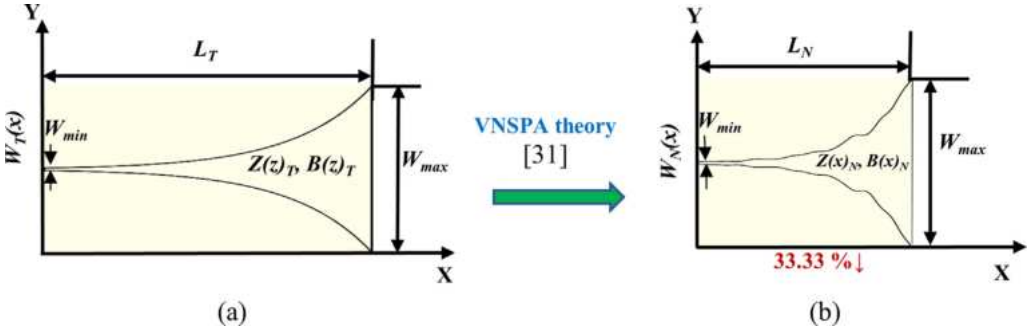

Fig. 2. (a) TSP and (b) NSP.

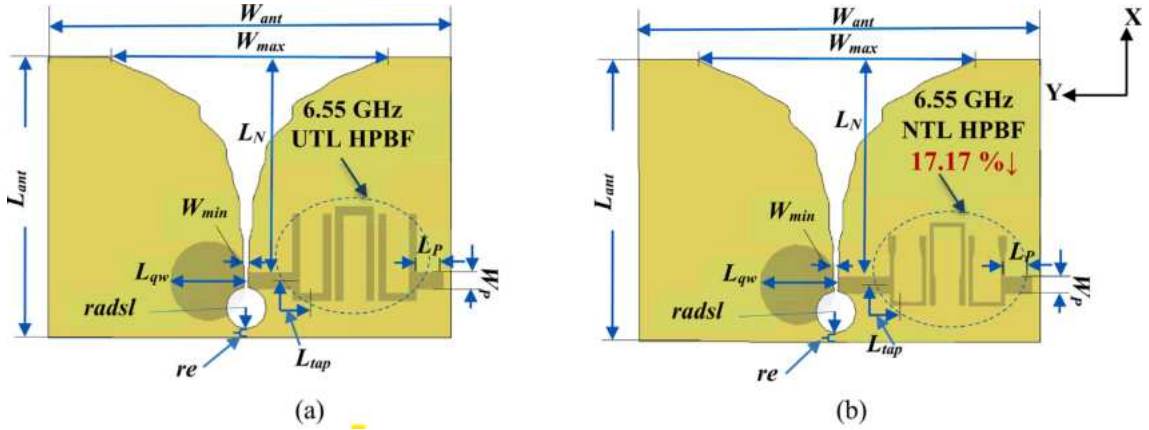

Fig. 3. Layouts of (a) Antenna 1 and (b) Antenna 2.

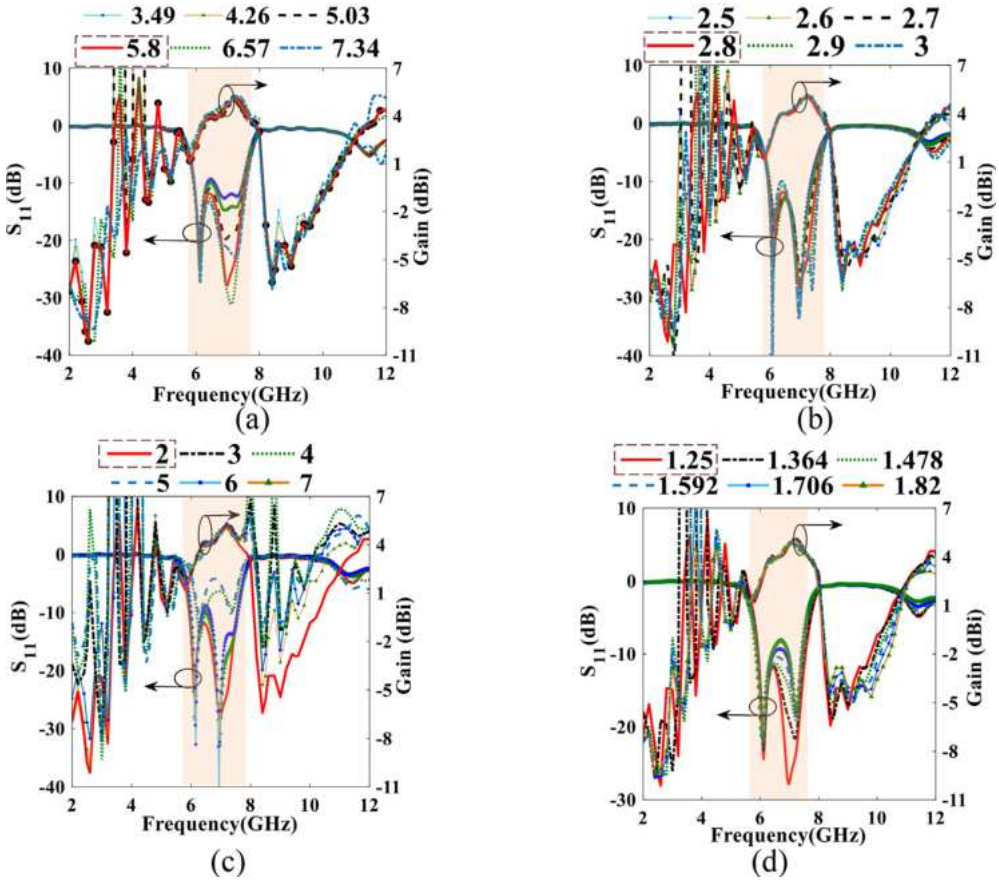

Fig. 4. S_{11} and gain parametric study of Antenna 1 on (a) L_{qw}, (b) L_{tap}, (c) L_p and (d) W_p.

Where A = 0.5 ∗ W_{min}, r is the taper rate, x is the position along L_T and C_n are the Fourier series coefficients which are optimized using built-in MATLAB function "fmincon" by reducing the following error function guaranteeing the equivalency of both profiles

$$\text{Error} = \sqrt{\frac{1}{M}\sum_{m=1}^{M}\frac{1}{4}\left(|A_N - A_T|^2 + Z(x)_T^{-2}|B_N - B_T|^2 + Z(x)_T^2|C_N - C_T|^2 + |D_N - D_T|^2\right)} \quad (3)$$

Where A_T, B_T, C_T and D_T are the ABCD matrix parameters of TSP. A_N, B_N, C_N, and D_N, are the ABCD matrix parameters of NSP and M is the number of the frequencies f_m (m = 1, 2, … M) within the UWB frequency band with frequency increment Δf.

Details on the design process, necessary constraints to get the appropriate NSP, and final optimization for UWB VNSA are provided in [31]. This study utilizes the simple compactness techniques of NTL [28,29,35–37] and VNSPA [31] theories to get a compact filtenna without degrading its performance, avoiding design difficulties and high costs. Fig. 3(a) and 3(b) show the layout of Antenna 1 and Antenna 2, respectively. L_{qw}, W_p, L_{tap}, L_p, *radsl*, W_{ant}, $L_{ant,}$ and *re* are the quarter wavelength, feeding port width, tapping length, the position from the feeding point, radius of slot, antenna width, antenna length, and the offset from the ground, respectively.

It should be mentioned here that the main parameters of Antenna 1 and 2 (L_N, W_{min}, W_{max}, L_p, *radsl*, W_{ant}, L_{ant} and *re*) are similar to the proposed UWB VNSA in [31] which indicates the effectiveness of employing the Vivaldi antenna for easy integration. However, different parametric studies on Antenna 1 and 2 are performed using CST software to overcome the mismatching between the VNSA feeding line and the inserted UTL and NTL HPBFs as shown in Fig. 4 and Fig. 5, respectively. Figs. 4(a) and 5(a) show that the impedance matching for Antenna 1 and 2, respectively is getting worse at L_{qw} < 5.8 mm (at L_{qw} = 3.49 mm (S_{11} < −9.33 dB and <−9.12 dB), L_{qw} = 4.26 mm (S_{11} < −9.92 dB and <−11.26 dB), and L_{qw} = 5.03 mm (S_{11} < −10.95 dB and <−13.21 dB)). Although the impedance matching at L_{qw} > 5.8 mm is getting better, L_{qw} = 5.8-mm (Antenna 1: S_{11} < −11.8 dB at 5.942–7.523 GHz with maximum realized gain of 5.15 dBi and Antenna 2:S_{11} < −15.26 dB at 5.924–7.48 GHz with maximum realized gain of 5.33 dBi) is selected for the compactness purpose and to guarantee that the main VNSA parameters are not changed due to the integration. As shown in Figs. 4(b) and 5(b), L_{tap} = 2.8 mm (S_{11} < −11.8 dB at 5.942–7.523 GHz with maximum realized gain of 5.15 dBi) and L_{tap} = 2 mm (S_{11} < −15.26 dB at 5.924–7.48 GHz with maximum realized gain of 5.33 dBi) are selected for Antenna 1 and 2 due to their better impedance matching than the optimized values for UTL HPBF [27] (L_{tap} = 2.9 mm (S_{11} < −10.86 dB)) and NTL HPBF [28,29] (L_{tap} = 2.9 mm (S_{11} < −8.48 dB)), respectively and other values. Although for Antenna 1 as shown in Fig. 4(b), the impedance matching at L_{tap} = 2.5 mm (S_{11} < −12.83 dB at 5.99–7.358 GHz), L_{tap} = 2.6 mm (S_{11} < −12.8 dB at 5.969–7.424 GHz) and L_{tap} = 2.7 mm (S_{11} < −12.42 dB at 5.955–7.486 GHz) is better, L_{tap} = 2.8 mm is selected due its 13.47 %, 7.97 %, and 3.16 % wider BW, respectively. For the feed line, the best impedance matching for both antennas is obtained at L_p = 2 mm as illustrated in Fig. 4(c) and 5(c). Finally, as shown in Fig. 4(d) and 5(d), the impedance matching for Antenna 1

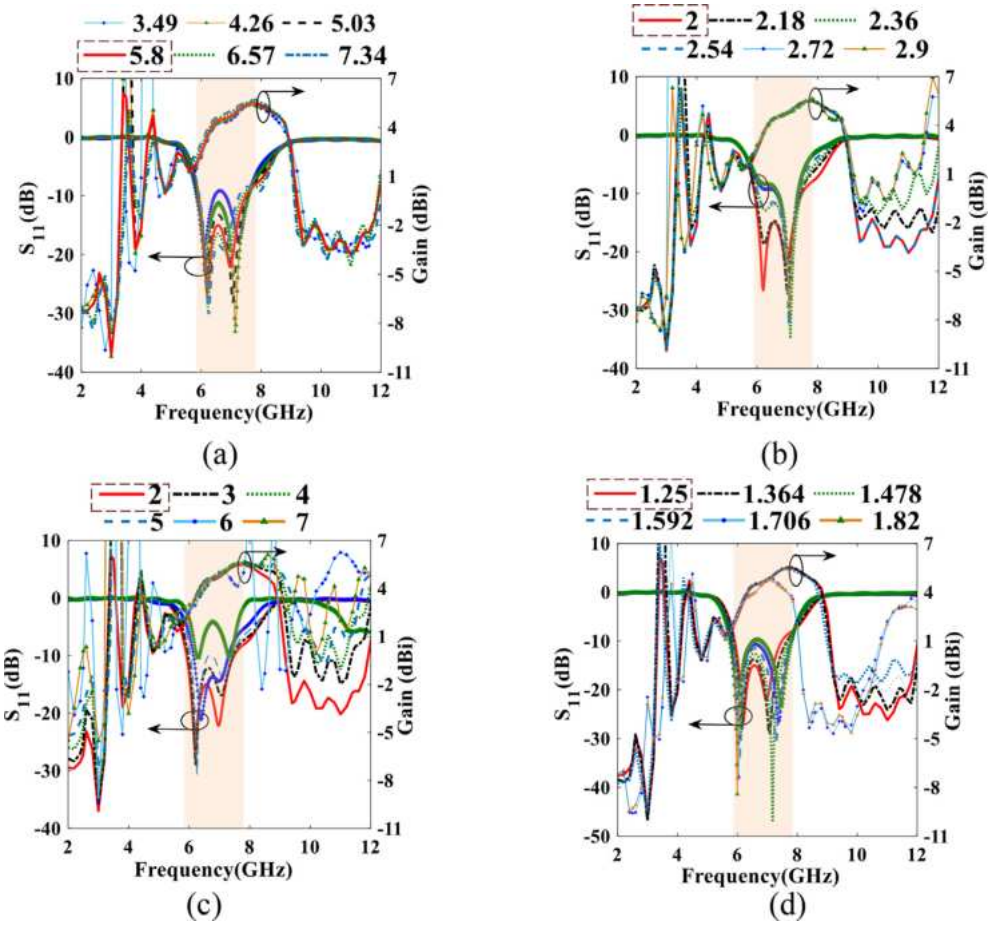

Fig. 5. S_{11} and gain parametric study of Antenna 2 on (a) L_{qw}, (b) L_{tap}, (c) L_p and (d) W_p.

Table 1
Calculated and implemented parameters of Antenna 1 and 2.

Parameters (mm)	Calculated	Optimized	
		Antenna 1	Antenna 2
W_{max}	24.45	21.03	21.03
L_T	25	$\boldsymbol{L_N}$ = 25	$\boldsymbol{L_N}$ = 25
L_{qw}	6.57	5.8	5.8
radsl	–	1.505	1.505
W_{min}	-	0.286	0.286
dis	–	24	24
re	–	0.5	0.5
W_{ant}	**–**	**29.8**	29.8
L_{ant}	**–**	**20.26**	20.26
L_{tap}	–	2.8	2
W_P	1.819	1.25	1.25
L_p	–	2	2

and 2 at W_p = 1.25 mm is better than the calculated one at 50 Ω, W_P = 1.82 mm (Antenna1: S_{11} < −8.15 dB at 5.860–7.416 GHz and Antenna 2: S_{11} < −9.77 dB at 5.753–7.8 GHz) and other values. The optimized results of Antenna 1 and 2 indicate that they provide wider BW than the 5G low-frequency band (5.975 GHz–7.12 5 GHz) by 27.26 % and 26.1 %, respectively. Table 1 illustrates the optimized parameters for both antennas. Based on the optimized parameters, the proposed filtennas are fabricated as shown in Fig. 6.

3. Results and discussions

The integration of 6.55 GHz UTL and NTL HPBFs into the novel compact linearly polarized UWB VNSA resulted in novel compact linearly polarized 6.55 GHz VNSFAs that are consistent with modern wireless system compactness requirements. The 17.17 % compactness in NTL HPBF of Antenna 2 provides more space to add the DC-biasing circuits in the reconfigurable antennas for CRNs applications Microwave network analyzer and anechoic chamber are used to measure the reflection coefficient and radiation properties of the proposed filtennas, respectively. Antenna1 and 2 provide measured results of S_{11} of <−10.35 dB and <−10.34 dB at 5.6–

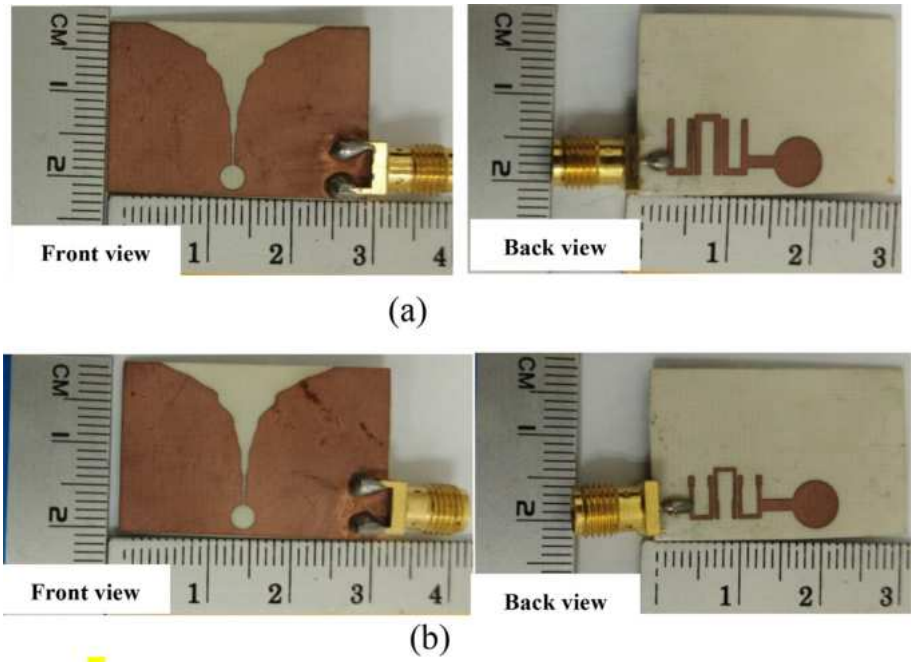

Fig. 6. Prototypes of (a) Antenna 1 and (b) Antenna 2.

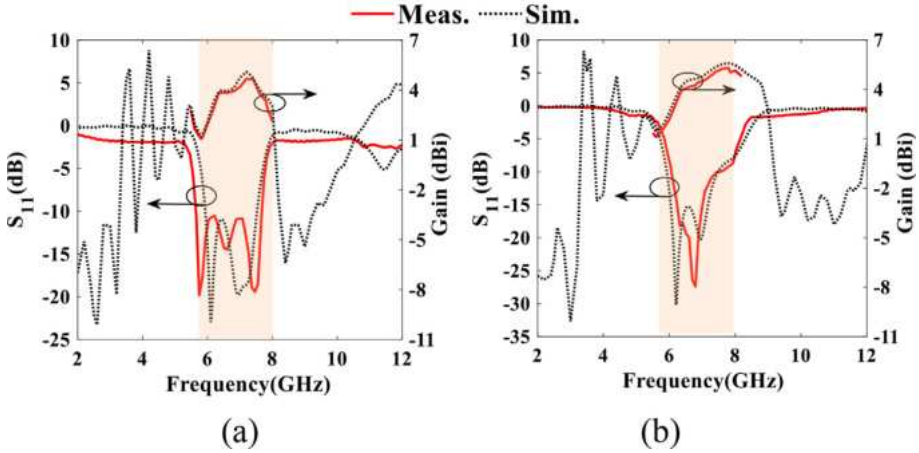

Fig. 7. Measured and simulated S_{11} and gain and of the proposed (a) Antenna 1 and (b) Antenna 2.

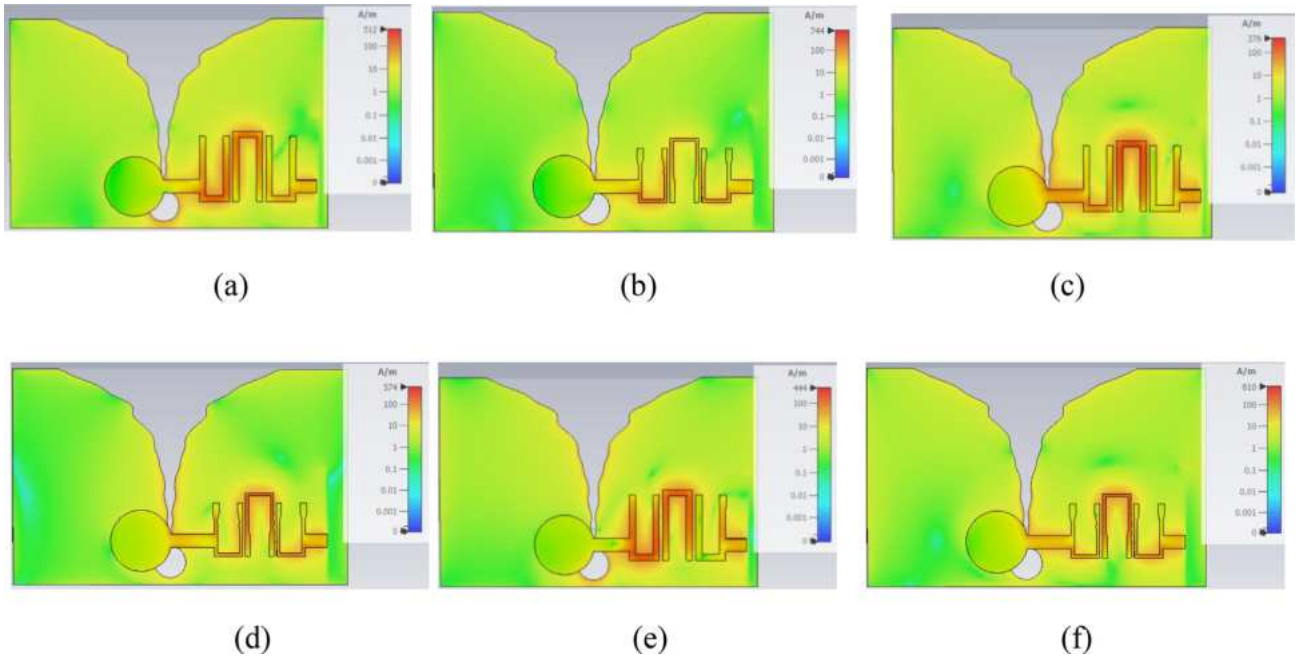

Fig. 8. Surface current distribution of Antenna 1 and Antenna 2 at f = (a),(b) 6 GHz, (c),(d) 6.85 GHz and (e) and (f) 7.35 GHz, respectively.

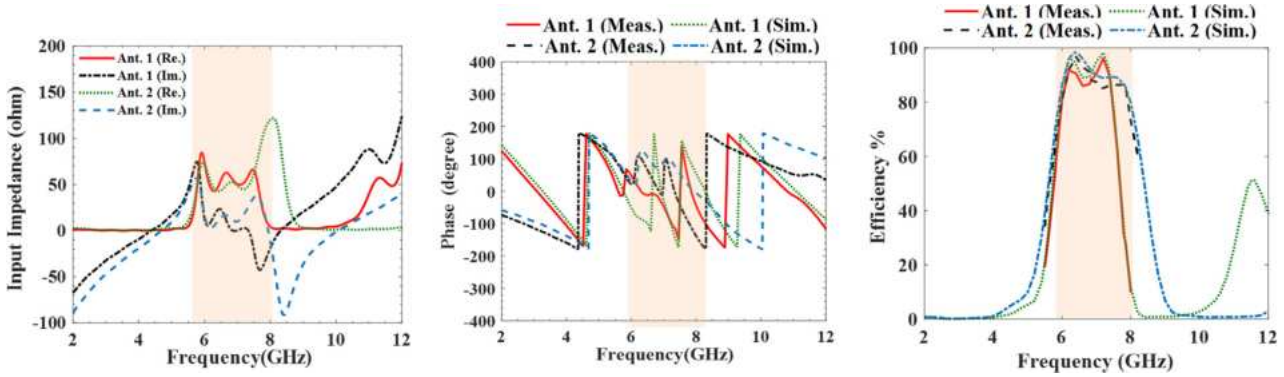

Fig. 9. (a) Simulated input impedance and (b) Measured and simulated total efficiency of the proposed filtennas.

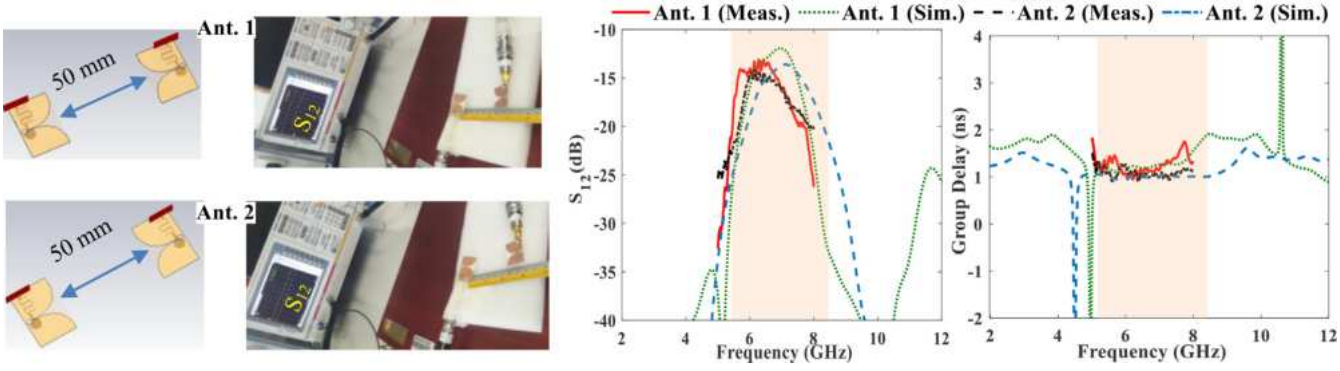

Fig. 10. (a) CST and measurement environments and simulated and measured (b) isolation and (c) F 2F group delay between the two samples of the proposed filtennas.

7.76 GHz and 6–7.76 GHz with peak realized gains of 4.84 dBi and 5.23 dBi, respectively as shown in Fig. 7. (a) and 7(b). The obtained BW of Antenna 1 and 2 is wider than 5.975–7.125 GHz by 46.76 % and 34.66 %, respectively. Also, it can be noticed that the maximum measured realized gain of Antenna 2 is higher than Antenna 1 by 5.16 % (Sim. = 3.4 %), which reflects the effectiveness of applying NTL theory [28,29,35–37] to reduce the length of UTL HPBFs' resonators by 17.17 %. This can be also explained by their current

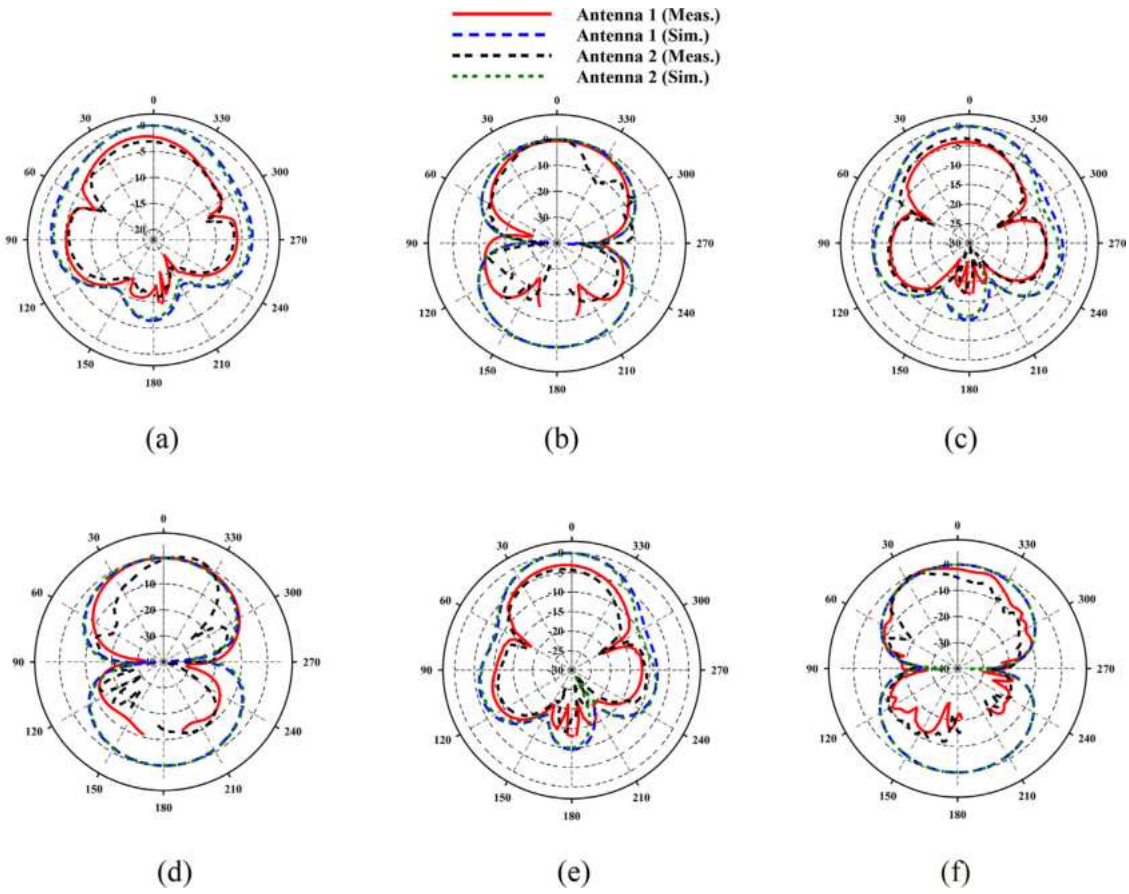

Fig. 11. Measured and simulated radiation pattern of Antenna 1 and Antenna 2 at 6 GHz (a) E and (b) H, 6.85 GHz (c) E and (d) H, and 7.35 GHz (e) E and(f)H.

Table 2
Other related filentennas at different frequency bands in the literature for the last three years.

Ref.	S11(dB) at Freq. Band (GHz), FBW	Gain (dBi)	Tot. Eff. (%)	Enhancement tech.	Size: $\lambda_0 \times \lambda_0$
This work	**Ant. 1:<−10.35, at 5.6–7.76, 32.33**	**4.96**	**53.92–95.2**	——	0.814 × **0.38**
	Ant. 2:<−10.34, at 6–7.76, 25.58	**5.23**	**81.04–96.16**	——	**0.6** × **0.41**
[26]	Ant. 1:<−13, at 5.48–7.73, 34.07	6.37	60.85–96.9	——	0.78 × 0.53
	Ant. 2:<−10.54, at 5.9–7.98,29.97	6.27	62.54–91.92	——	0.84 × 0.57
[9]	<−12at 2.32–2.55, 9.45	3.14	NA	——	0.54 × 0.58
[11]	<−10.54 at 25.99– 31.49, 19.14	8.84	Sim. 84.9	parasitic and slits	3.15 × 1.49
[12]	<−11.45 at 1.01–1.96, 61.2	2.96	86–93	Use of via	3.1 × 0.16
[17]	<−10.67 at 3.45–3.81, 9.92	7.5	NA	——	0.61 × 0.61
[19]	<−10.89 at 6.3–9.1, 37.11	8.65	NA	Use of via	NA
[18]	<−14.1 at 2.42–2.52,0.4.05	6.6	0.9	Use of via	0.361 × 0.426
[14]	<−11.23 at 2.31–2.49, 7.5	0.74	NA	——	0.28 × 0.24

*Tot. Eff.: Total efficiency, NA: Not available and tech.: techniques.

distribution in Fig. 8 where the current distribution at the NTL HPBF of Antenna 2 is higher than that at UTL HPBF of Antenna 1 at f = 6 GHz, f = 6.85 GHz and f = 7.35 GHz. Despite the 51.94 % size reduction in Antenna 1 and 2, they provide a moderate maximum realized gain of 4.96 dBi and 5.23 dBi, respectively. This demonstrates the effectiveness of using the simple and low-cost compactness techniques of NTL [28,29,35–37] and VNSPA [31] theories in reducing the filtenna size without degrading its performance. The good impedance matching of both filtennas is also illustrated in Fig. 9(a) where the real and imaginary parts of the simulated input impedance are oscillating around 50 Ω and 0 Ω, respectively. According to Fig. 9(b), the phase is leading in Antenna 2′s NTL HPBF because the signal will travel a longer distance through Antenna 1′s UTL HPBF. As depicted in Fig. 9(c), the measured total radiation efficiencies for antennas 1 and 2 are between 53.92 % and 95.27 % (Sim. between 60 % and 98.31 %) and 81.04 % and 96.16 % (Sim. between 86.4 % and 98.21 %), respectively. Fig. 10(a) shows the simulation and measurement setups to calculate face to face (F 2F) group delay of both antennas. The isolation between two samples at a distance of 50 mm is <−12 dB as indicated in Fig. 10(b). Fig. 10(c) shows that, the approximate flat measured group delays are around 1.25 ns and 1 ns for Antenna 1 and 2, respectively. The group delay in Antenna 2 is smaller than that in Antenna 1 due to the 17.17 % compactness in its NTL HPBF as compared to UTL HPBF in Antenna 1 by which the signal will take the longer path passing through the UTL HPBF. For both VNSFAs, Fig. 11(a) and (b), (c) and (d), and (e) and (f), compare the measured and simulated normalized 2-D polar plots E-plane (XY-plane) and H-plane (XZ-plane) radiation patterns at f = 6 GHz, f = 6.85 GHz and f = 7.35 GHz with semi end-fire (inverted pear-like) and semi dipole shapes,

respectively. This directive property along with the moderate gain and small size make the proposed filtennas good candidates for high-resolution applications such as breast cancer detection. The discrepancy between the simulated and measured results is due to fabrication tolerance, lab and human errors, imperfect soldering of SMA connectors, and the difference between the simulation and real measurement environments. The enhanced performance provided by these 5G VNSFAs, in addition to their 51.94 % size reduction, makes them the ideal candidate for the rapidly emerging 5G mobile communication applications in which compact RF circuits and antennas with good performances are highly desirable.

Finally, Table 2 compares the proposed linearly polarized filtennas to the most recent relevant work in the literature. As compared to the recent work in [26], although 51.94 % size reduction is obtained simply using VNSPA theory [31], the proposed VNSFAs provide good wideband impedance matching, efficiencies, and moderate high gains. As compared to the works using enhancement techniques, the proposed filtennas are smaller than [11,18] and [12] with better FBW, gain and efficiency, respectively. It should also be noted that the proposed linearly polarized VNSFAs are the smallest among the others in the literature except [14] which suffers from low FBW and gain. Without using enhancement techniques, the proposed linearly polarized VNSFAs are better than [9] in terms of FBW and gain. Also, they are smaller in size and have better FBW than [17] although of its higher gain.

4. Conclusion

Two compact linearly polarized 5G VNSAFs with stable radiation patterns and moderate gains are designed in this work effectively using a co-design approach by integrating the predesigned 5G UTL and NTL HPBFs with compact UWB VNSA exploiting its compact size and good performance in terms of high gain, wide BW and stable radiation patterns. The proposed linearly polarized filtennas provide good measured S_{11} of <−10 dB with 46.76 % (Antenna 1) and 34.66 % (Antenna 2) enhanced BW than 5.975–7.125 GHz. These 5G VNSFAs' outstanding performance, together with their 51.94 % size reduction, make them more desirable for wireless communication applications such as 5G mobile phones and Wi-Fi. Additionally, the proposed 6.55 GHz VNSFA using NTL HPBF provides both compactness and opportunity to be used in CRNs providing more space for switching diodes and the DC-biasing circuit components (DC-blocking capacitors, biasing inductors, biasing lines, and pads). Compact NTL IBFs can be exploited as future work for more compactness, wider BW, and higher harmonics suppression.

Declaration of Competing Interest

The authors declare that they have no known competing financial interests or personal relationships that could have appeared to influence the work reported in this paper.

Acknowledgment

The authors would like to acknowledge Enterprise Ireland, Ireland for providing financial assistance. We also would like to thank **Mr. Sean Keys** for his effort in collecting the required data.

References

[1] Anguera J, Andújar A, Huynh M-C, Orlenius C, Picher C, Puente C. Advances in antenna technology for wireless handheld devices. Int J Antennas Propag 2013;2013:1–25. doi: https://doi.org/10.1155/2013/838364.
[2] An H, Nauwelaers B, Van De Capelle A. A new approach of broadband microstrip antenna design. IEEE Antennas Propagat Soc AP-S Int Symp (Digest) 1992:475–8. doi: https://doi.org/10.1109/APS.1992.221898.
[3] Abbaspour-Tamijani A, Rizk J, Rebeiz G. Integration of filters and microstrip antennas. IEEE Antennas Propagat Soc, AP-S Int Symp (Digest) 2002;2:874–7. doi: https://doi.org/10.1109/aps.2002.1016784.
[4] Gangwar AK, Alam MS, Rajpoot V, Ojha AK. Filtering antennas: a technical review. Int J RF Microwave Comput-Aided Eng 2021;31:1–31. doi: https://doi.org/10.1002/mmce.22797.
[5] Sahu B, Singh S, Meshram MK, Singh SP. A new compact ultra-wideband filtering antenna with improved performance. J Electromagn Waves Appl 2019;33:107–24. doi: https://doi.org/10.1080/09205071.2018.1529630.
[6] Jiang ZH, Werner DH. A compact, wideband circularly polarized co-designed filtering antenna and its application for wearable devices with low SAR. IEEE Trans Antennas Propag 2015;63:3808–18. doi: https://doi.org/10.1109/TAP.2015.2452942.
[7] Jiang ZH, Gregory MD, Werner DH. Design and experimental investigation of a compact circularly polarized integrated filtering antenna for wearable biotelemetric devices. IEEE Trans Biomed Circuits Syst 2016;10:328–38. doi: https://doi.org/10.1109/TBCAS.2015.2438551.
[8] Cheng W. Compact 2.4-GHz filtering monopole antenna based on modified SRR-inspired high-frequency-selective filter. Optik (Stuttg) 2016;127:10653–8. doi: https://doi.org/10.1016/j.ijleo.2016.08.086.
[9] Cheng W, Li D. Compact filtering monopole antennas based on the miniaturised coupled filter. In: 2018 Cross strait quad-regional radio science and wireless technology conference, CSQRWC 2018; 2018. p. 15–17. doi: 10.1109/CSQRWC.2018.8455341.
[10] Hu HT, Chen FC, Chu QX. Novel broadband filtering slotline antennas excited by multimode resonators. IEEE Antennas Wirel Propag Lett 2017;16:489–92. doi: https://doi.org/10.1109/LAWP.2016.2585524.
[11] Yang K, Hoang MH, Bao X, McEvoy P, Ammann MJ. Dual-stub Ka-band Vivaldi antenna with integrated bandpass filter. IET Microwaves Antennas Propag 2018;12:668–71. doi: https://doi.org/10.1049/iet-map.2017.0488.
[12] Sahu B, Singh S, Meshram MK, Singh SP. Integrated design of filtering antenna with high selectivity and improved performance for L-band applications. AEU-Int J Electron C 2018;97:185–94. doi: https://doi.org/10.1016/j.aeue.2018.10.015.
[13] Tang MC, Chen Y, Ziolkowski RW. Experimentally validated, planar, wideband, electrically small, monopole filtennas based on capacitively loaded loop resonators. IEEE Trans Antennas Propag 2016;64:3353–60. doi: https://doi.org/10.1109/TAP.2016.2576499.
[14] Pal P, Sinha R, Mahto SK. Synthesis approach to design a compact printed monopole filtenna for 2.4 GHz Wi-Fi application. Int J RF Microwave Comput Aided Eng 2021;31:2–9. doi: https://doi.org/10.1002/mmce.22619.
[15] Tang H, Chen JX, Chu H, Zhang GQ, Yang YJ, Bao ZH. Integration design of filtering antenna with load-insensitive multilayer Balun filter. IEEE Trans Compon Packaging Manuf Technol 2016;6:1408–16. doi: https://doi.org/10.1109/TCPMT.2016.2600541.
[16] Cui J, Zhang A, Yan S. Co-design of a filtering antenna based on multilayer structure. Int J RF Microwave Comput-Aided Eng 2020;30:1–6. doi: https://doi.org/10.1002/mmce.22096.
[17] Wang W, Ran J, Hu N, Xie W, Wu Y, Kishk AA. A novel differential filtering patch antenna with high selectivity. Int J RF Microwave Comput-Aided Eng 2019;29:1–10. doi: https://doi.org/10.1002/mmce.21880.
[18] Zheng Z, Li D, Tan X, Wang M, Deng Y. Compact low-profile differential filtering microstrip patch antenna with high selectivity and deep rejection using single-layer substrate. IEEE Access 2021;9:76047–55. doi: https://doi.org/10.1109/ACCESS.2021.3080309.
[19] Feng W, Feng Y, Wu LS, Shi Y, Zhou XY, Che W. A novel leaky wave endfire filtering antenna based on spoof surface plasmon polaritons. IEEE Trans Plasma Sci 2020;48:3061–6. doi: https://doi.org/10.1109/TPS.2020.3013608.
[20] Juma'a FK, Al-Mayoof AI, Abdulhameed AA, Alnahwi FM, Al-Yasir YIA, Abd-Alhameed RA. Design and implementation of a miniaturized filtering antenna for 5G mid-band applications. Electronics (Switzerland) 2022;11:. doi: https://doi.org/10.3390/electronics11929792979.
[21] Ramahatla K, Mosalaosi M, Yahya A, Basutli B. Multiband reconfigurable antennas for 5G wireless and CubeSat applications: a review. IEEE Access 2022;10:40910–31. doi: https://doi.org/10.1109/ACCESS.2022.3166223.
[22] Haider A, Rahman MU, Naghshvarianjahromi M, Kim HS. Time-domain investigation of switchable filter wide-band antenna for microwave breast imaging. Sensors (Switzerland) 2020;20:1–10. doi: https://doi.org/10.3390/s20154302.
[23] Awan WA, Hussain N, Kim S, Kim N. A frequency-reconfigurable filtenna for GSM, 4G-LTE, ISM, and 5G sub-6 GHz band applications. Sensors 2022;22:5558. doi: https://doi.org/10.3390/s22155558.
[24] Ibrahim AA, Mohamed HA, Rizo ARD, Parra-Michel R, Aboushady H. Tunable filtenna with DGS loaded resonators for a cognitive radio system based on an SDR transceiver. IEEE Access 2022;10:32123–31. doi: https://doi.org/10.1109/ACCESS.2022.3160467.
[25] Abdullah LW, Sallomi AH, Jassim AK. A reconfigurable dual port antenna system for underlay/interweave cognitive radio. Int J Electrical Comput Eng 2023;13:443–53. doi: https://doi.org/10.11591/ijece.v13i1.pp443-453.
[26] Saleh S, Jamaluddin MH, Alali B, Althuwayb AA. Compact 5G Vivaldi tapered slot filtering antenna with enhanced bandwidth. Comput Mater Continua 2023;74:5983–99. doi: https://doi.org/10.32604/cmc.2023.035585.
[27] Saleh S, Ismail W, Zainal Abidin IS, Jamaluddin MH. 5G Hairpin and interdigital bandpass filters. Int J Integr Eng 2020;12:71–9. doi: https://doi.org/10.30880/ijie.2020.12.06.009.

[28] Saleh S., Ismail W., Zainal Abidin I.S., Jamaluddin M.H., Al-Gailani S.A., Bataineh M.H., et al. Size reduction percentage study of 5g hairpin bandpass filter nonuniform transmission line resonator. In: APACE 2019–2019 IEEE Asia-Pacific conference on applied electromagnetics, proceedings; 2019. doi: 10.1109/APACE47377.2019.9021071.
[29] Saleh S, Ismail W, Zainal Abidin IS, Jamaluddin MH. Compact 5G hairpin bandpass filter using non-uniform transmission lines theory. Appl Comput Electromagn Soc J 2021;36. doi: https://doi.org/10.47037/2020.ACES.J.360202.
[30] Saleh S, Ismail W, Abidin ISZ, Jamaluddin MH, Bataineh MH, Zainal Abidin IS. Compact UWB Vivaldi tapered slot antenna. Alex Eng J 2022;61:4977–94. doi: https://doi.org/10.1016/j.aej.2021.09.055.
[31] Saleh S, Ismail W, Zainal Abidin IS, Jamaluddin MH, Bataineh MH, Al-Zoubi AS. Novel compact UWB Vivaldi nonuniform slot antenna with enhanced bandwidth. IEEE Trans Antennas Propag 2022;70(8):6592–603.
[32] Saleh S, Ismail W, Zainal Abidin IS, Jamaluddin MH, Bataineh M, Alzoubi A. Compact reconfigurable ultra wide band and 5G narrow band vivaldi tapered slot antenna. In: 2020 IEEE international RF and microwave conference, RFM 2020. p. 32–5. doi: https://doi.org/10.1109/RFM50841.2020.9344743.
[33] Saleh S, Jamaluddin MH, Razzaz F, Saeed SM. Compact 5G nonuniform transmission line interdigital bandpass filter for 5G/UWB reconfigurable antenna. Micromachines (Basel) 2022;13:1–15.
[34] Hong J-S-G, Lancaster MJ. Microstrip filters for RF/microwave applications. John Wiley & Sons; 2011.
[35] Saleh S, Alzoubi A, Bataineh M. Compact UWB unequal split Wilkinson power divider using nonuniform transmission lines. In: 2018 International conference on computer, control, electrical, and electronics engineering, ICCCEEE 2018; 2018. doi: 10.1109/ICCCEEE.2018.8515887.
[36] Saleh S, Ismail W, Zainal Abidin IS, Jamaluddin MH, Al-Gailani SA, Alzoubi AS, et al. Nonuniform compact Ultra-Wide Band Wilkinson power divider with different unequal split ratios. J Electromagn Waves Appl 2020;34(2):154–67.
[37] Saleh S, Ismail W, Zainal Abidin IS, Jamaluddin MH, Al-Gailani SA, Alzoubi AS, et al. Compact UWB 1:2:1 unequal-split 3-way bagley power divider using non-uniform transmission lines. J Electromagn Waves Appl 2021;35(2):262–76.

Sahar Saleh is a Postdoctoral Researcher in 5G RF at WiSAR Lab, ATU Donegal. Sahar received her bachelor's degree in electronics and communication engineering from Aden University, Yemen, an MSc degree in wireless communications engineering from Yarmouk University, Jordan, and a Ph.D. in microwave and satellite systems from Universiti Sains Malaysia. In 2012, Sahar joined the Faculty of Engineering at Aden University as a Laboratory Technician and Junior Lecturer and following that, worked as a research assistant with Universiti Sains Malaysia. Before joining WiSAR, Sahar worked as a Postdoctoral fellow at the Wireless Communication Center, Universiti Teknologi Malaysia, Johor, Malaysia. Dr. Saleh's research interests include the miniaturization of RF/Microwaves components (filters, dividers, and antennas), wearable antennas, 3D antennas, MIMO, Internet of Healthcare Things (IoHT).

Nick Timmons (MIEEE) holds a Ph.D (2011) in Wireless Body Area Networks from Queen's University Belfast, an M.Sc (1994) in Satellite Engineering Design from the University of Surrey, and a B.Eng (Hons)(1989) from the University of Ulster, Jordanstown. He joined Atlantic Technological University (LyIT) in 1997 is co-founder and Academic Director of the WiSAR Lab. Prior to that he had 10 years industrial experience as an RF engineer including roles in research for Connaught Electronics (Valeo) leading the development of low power RF transceivers for the automobile industry, and as a Senior Principal RF Engineer in Siemens working on Satellite Communications RF/microwave design. His current research interests are in the areas of Wireless Sensor Networks (WSNs), 5G and beyond, Body Area Networks (BAN), wearable antenna design, ultra-Low Power Communication Protocols: MAC and Network/Routing protocols.

Jim Morrison (MIEEE) holds a PhD (2006) in Digital Security from the University of Limerick, an MSc (1992) in Industrial Applications of Computing from the Open University and a BEng (1981) in Electronics and Electrical Engineering from Queens University of Belfast. He has been a member of the IEEE over 30 years. He joined ATU in 1985 and is currently Head of Department of Electronics and Mechanical Engineering. He is a co-founder of the WiSAR Lab. His current research interests are in the area of Embedded Wireless Systems with a focus on wearable sensor applications.

Widad Ismail (M'04) received the bachelor's (Hons.) degree in electronics and communication engineering from the University of Huddersfield, U.K., in 1999, and the Ph.D. degree (Active Integrated Antenna with Image Rejection) in electronics and communication engineering from the University of Birmingham, U.K., in 2004. She is currently a Professor and a Project Coordinator with the AutoID Laboratory, Universiti Sains Malaysia. Her main areas of research are wireless system design, RFID, active integrated antennas, and RF and microwave systems engineering. She is a member of the Wireless World Research Forum